Correlation of high PRDX4 expression with poor prognosis in patients with ESCA: Bioinformatics and *in vitro* validation

XING LIU[1], LANLAN PAN[2], HUICHAO SONG[1] and WENYAN PAN[3]

[1]Department of Emergency, The Second People's Hospital of Futian District Shenzhen, Shenzhen, Guangdong 518049, P.R. China;
[2]Neurology Department, Helan People's Hospital, Yinchuan, Ningxia Hui Autonomous Region 750200, P.R. China;
[3]Department of Radiotherapy, General Hospital of Ningxia Medical University, Yinchuan, Ningxia Hui Autonomous Region 750003, P.R. China

Received January 20, 2026; Accepted September 1, 2026

DOI: 10.3892/mco.2026.2976

Abstract. Esophageal cancer (ESCA) is a highly lethal gastrointestinal malignancy with limited therapeutic options. The peroxiredoxin 4 (PRDX4) protein has antioxidant functions and is implicated in various types of cancer, but its role in ESCA remains poorly understood. The purpose of the present study was to investigate PRDX4 expression in ESCA, evaluate its clinical prognostic value, and explore associations with the tumor immune microenvironment and metabolic pathways, with validation by immunohistochemistry (IHC). PRDX4 expression in ESCA was analyzed using UALCAN, SANGERBOX, TIMER, STRING and Kaplan-Meier Plotter databases. IHC was performed on 60 ESCA and matched normal tissues. Associations with overall survival (OS), progression-free interval (PFI), disease-specific survival (DSS), disease-free interval (DFI), TNM stage and immune cell infiltration were examined. Gene Ontology and Kyoto Encyclopedia of Genes and Genomes enrichment analyses were conducted. PRDX4 was significantly upregulated in ESCA tissues (P<0.05). IHC showed strong positive staining in all 60 tumor tissues vs. 11/60 normal tissues (P<0.05). High PRDX4 expression correlated with poorer OS [Hazard ratio (HR)=1.82; 95% confidence interval (CI): 1.21-2.74; P=0.004], PFI (HR=1.65; 95% CI: 1.08-2.52; P=0.019) and DSS (HR=2.01; 95% CI: 1.32-3.06; P<0.001), but not with DFI (P=0.35). PRDX4 levels differed significantly across N stages (P=0.006), but not T or M stages. Furthermore, PRDX4 expression was significantly associated with tumor differentiation (P=0.028) and showed a trend towards larger tumor size (P=0.061). PRDX4 expression correlated with infiltration of dendritic cells, macrophages, $CD8^+$ T cells, regulatory T cells, M1 macrophages and activated mast cells. Gene Ontology/Kyoto Encyclopedia of Genes and Genomes pathways included mitochondrial function, carbon metabolism, tricarboxylic acid cycle and pyruvate metabolism. Protein interaction analysis showed associations with GPX3 and TXN. PRDX4 represents a potential prognostic biomarker for ESCA, with additional diagnostic value suggested by Receiver Operating Characteristic analysis (Area Under Curve=0.969). In conclusion, PRDX4 is significantly overexpressed in ESCA and is associated with poor prognosis, lymph node metastasis, immune infiltration and metabolic reprogramming. The present findings suggest that PRDX4 may serve as a promising prognostic biomarker and a potential therapeutic target for ESCA.

Introduction

The PRDX family is a novel protein family with crucial antioxidant functions, widely expressed in various organisms (1). The encoded proteins function primarily as antioxidant enzymes belonging to the peroxiredoxin family, localized within the cytoplasm. Peroxidases in this family utilize reducing equivalents derived from thiol-containing donors to reduce hydrogen peroxide and alkyl hydroperoxides into water and alcohols (2), playing a regulatory role in the activation of the transcription factor NF-kappa B (3). Peroxiredoxin 4 (PRDX4) regulates oxidative protein folding by anchoring to the endoplasmic reticulum and exerts antioxidant effects through secretion into the extracellular matrix, displaying relatively complex and diverse functions across different tumor cells (4).

Esophageal cancer (ESCA) is a common malignant tumor, with squamous cell carcinoma (ESCC) being the predominant histological type in China (5). Despite significant advancements in diagnosis and treatment, the five-year survival rate for patients with ESCA remains ~20% (6). Tumor metastasis is a major factor contributing to patient mortality; however, its mechanisms remain unclear (7). Therefore, investigating the mechanisms underlying ESCA metastasis is essential for improving patient prognosis.

Previous studies have demonstrated that PRDX4 is a multifunctional protein involved in preventing oxidative damage, regulating cell proliferation and intracellular signaling, and contributing to tumor malignant progression, recurrence and

Correspondence to: Professor Wenyan Pan, Department of Radiotherapy, General Hospital of Ningxia Medical University, 804 Shengli South Street, Xingqing, Yinchuan, Ningxia Hui Autonomous Region 750003, P.R. China
E-mail: lovelypenguin1023@163.com

Key words: esophageal cancer, peroxiredoxin 4, prognosis, immunohistochemistry, bioinformatics, prognostic biomarker

death (8-10). Specifically, PRDX4 has been implicated in promoting proliferation and migration in ESCA cells through the lncRNA THUMPD3-AS1/miR-29a-3p/ELK1 signaling pathway, as reported in a recent study (11). However, despite these mechanistic insights, a comprehensive evaluation of PRDX4's clinical significance, its correlation with the tumor immune microenvironment (TIME), and its impact on metabolic pathways in ESCA remains lacking. Furthermore, the prognostic value of PRDX4 protein expression validated by immunohistochemistry (IHC) in ESCA cohorts has not been systematically reported.

Therefore, the gap aimed to be filled by the present study is 3-fold: i) to validate the overexpression of PRDX4 at both the mRNA and protein levels in a clinical ESCA cohort; ii) to comprehensively assess its prognostic value and clinicopathological correlations, particularly with lymph node metastasis; and iii) to explore its potential biological functions in ESCA through multi-omics bioinformatics analysis, focusing on immune infiltration and metabolic pathways. Thus, the present study investigated the expression of PRDX4 in ESCA and its relationship with prognosis from a bioinformatics perspective, further validating the findings through *in vitro* experiments.

Materials and methods

Materials. Archived ESCA tissues and normal esophageal mucosal specimens were collected from the Department of Pathology, Tumor Hospital of Ningxia Medical University General Hospital (Yinchuan, China), between January 2023 and December 2024. A total of 112 cases with complete medical records and comprehensive clinical data were initially selected. After excluding patients with a history of radiotherapy or chemotherapy prior to tissue sampling, 60 cases remained for inclusion in the present study. The cohort comprised 41 male and 19 female patients, with a median age of 46 years (range, 35-74 years). All pathological indicators were re-evaluated independently by two pathologists, and consensus was achieved. The present study was approved by the Ethics Committee of Ningxia Medical University General Hospital (approval no. KYLL-2026-0022; Yinchuan, China).

Database materials. A uniformly normalized pan-cancer dataset (TCGA TARGET GTEx; PANCAN, N=19,131, G=60,499) was downloaded from the UCSC database (https://xenabrowser.net/), from which PRDX4 gene expression data were extracted for all samples. Sample selection was limited to six predefined source categories: Solid Tissue Normal, Primary Solid Tumor, Primary Tumor, Normal Tissue, Primary Blood-Derived Cancer (Bone Marrow), and Primary Blood-Derived Cancer (Peripheral Blood). Expression values were then transformed using the formula $\log_2(x + 0.001)$. Cancer types with fewer than three samples were subsequently excluded, resulting in the inclusion of expression data for 34 distinct cancer types.

UALCAN database. The UALCAN database (https://ualcan.path.uab.edu/analysis.html) is an online bioinformatics tool primarily designed for cancer-related gene expression analysis (12). It provides multiple datasets and analytical tools to help researchers understand the molecular characteristics of various cancers. The main functions of UALCAN include gene expression, survival, tumor staging, grading, and subgroup analyses based on clinical characteristics, enabling detailed investigation of potential therapeutic targets and biomarkers.

SANGERBOX database. The SANGERBOX database (http://sangerbox.com/home.html) is an interactive, web-based bioinformatics tool platform integrating multiple databases (13). It facilitates rapid batch processing of data, reducing user difficulty and enhancing analytical efficiency. Analysis steps were as follows: i) pan-cancer analysis; ii) prognostic analysis of gene expression; iii) input gene: PRDX4; sample source selection: all samples; data source: TCGA + GTEx; survival data: Overall survival (OS), progression-free interval (PFI), disease-free interval (DFI) and disease-specific survival (DSS).

STRING database. The STRING database (https://string-db.org/) is a widely used tool for analyzing gene and protein interactions (14). Interaction data within this database originate from high-throughput experimental data, computational genomic predictions, automated text mining, and other databases. Currently, STRING is among the most comprehensive resources for protein-protein interaction (PPI) analysis, encompassing a broad range of species and an extensive dataset. It integrates both experimentally validated and computationally predicted interactions. Search parameters for the present study were set as follows: i) select 'protein by name'; ii) input 'PRDX4' into the 'Protein names' field; iii) choose 'Homo sapiens' for 'Organism'.

TIMER database. The TIMER database (https://cistrome.shinyapps.io/timer/) analyzes immune cell infiltration in tumor tissues based on high-throughput sequencing (RNA-Seq expression profiling) data (15). It primarily provides infiltration profiles for six immune cell types: B cells, $CD4^+$ T cells, $CD8^+$ T cells, neutrophils, macrophages and dendritic cells (DCs).

KM-PLOTER database. The Kaplan-Meier Plotter (https://www.kmplot.com/analysis/) database is widely used for survival analysis (16), sourcing data from GEO, EGA and TCGA databases. It contains data for analyzing 54,675 genes and 18,674 cancer samples, enabling the assessment of the impact of over 54,000 genes on patient survival across 21 cancer types.

Table SI database. Clinicopathological data for patients with ESCA were obtained from The Cancer Genome Atlas (TCGA) ESCA dataset (n=185). Gene expression data (RNA-Seq) and corresponding clinical annotations were downloaded from the UCSC Xena browser (https://xenabrowser.net/). PRDX4 expression values were log2-transformed $[\log_2(TPM + 1)]$ for analysis. Definitions of variables are as follows: PRDX4 expression groups: Patients were divided into high- and low-expression groups based on the optimal cutoff value (6.786 for OS) determined by the maxstat R package (Maximally Selected Rank Statistics, version 0.7-25), with minimum and maximum sample sizes per group set at >25 and <75%, respectively, to minimize bias. Histologic grade (tumor differentiation): Defined according to the TCGA clinical annotation, following the World Health Organization (WHO) histological tumor classification: Grade I: Well differentiated; Grade II: Moderately differentiated; Grade III: Poorly differentiated; Grade IV/GX: Undifferentiated or grade not determined. Tumor size: Defined as the maximum diameter of the primary tumor (in cm), as recorded in the TCGA clinical

dataset. A cutoff of 4 cm was used to stratify patients into smaller (<4 cm) and larger (≥4 cm) tumor groups, consistent with previous ESCA studies.

Sample sizes: A total of 162 patients with complete PRDX4 expression data and available clinicopathological information were included in this analysis (81 in the low-expression group and 81 in the high-expression group). The sample size for each subgroup is shown in Table SI. These numbers are consistent with the TCGA-ESCA cohort characteristics reported in a previous study (17).

IHC. Tissue sections (4-micrometer-thick) were obtained from 60 cases of esophageal carcinoma and corresponding normal esophageal mucosal tissues. The Multimer method was employed to stain tissues using the Benchmark XT Roche IHC instrument, with heat-induced antigen retrieval conducted using EDTA (pH 9.0). Slides were incubated with rabbit anti-human PRDX4 antibody (Zhengneng Biotechnology Co., Ltd.; diluted 1:800) at 37˚C for 30 min, followed by incubation with a horseradish peroxidase-labeled secondary antibody (ZSGB-BIO PV8000D) at 37˚C for 32 min. Sections were then stained with diaminobenzidine (DAB) and counterstained with hematoxylin. Positive PRDX4 staining was localized in the cytoplasm, presenting colors ranging from faint yellow to tan-brown. The proportion of tumor cells with positive cytoplasmic staining for PRDX4 was evaluated under a light microscope. Evaluation was conducted in 10 randomly selected, non-overlapping high-power fields (x400 magnification) and scored based on the percentage of positive cells and staining intensity as follows: No staining, 0 points; positive cell rate ≤50% with light tan-brown staining, 1 point; positive cell rate 50-100% with light tan-brown staining, 2 points; positive cell rate ≤50% with tan-brown staining, 3 points; positive cell rate 50-100% with tan-brown staining, 4 points; positive cell rate ≤50% with dark brown staining, 5 points; positive cell rate 50-100% with dark brown staining, 6 points. Scores of 0-2 indicated negative (-), 3-4 indicated positive (+), and 5-6 indicated strongly positive (++). This scoring system, while comprehensive, may be simplified in future clinical applications by using a binary (positive/negative) or a three-tier (negative, moderate, strong) system to enhance its clinical utility.

Statistical analysis. Statistical analyses were performed using R software (https://www.R-project.org/.version 4.2.2). mRNA expression data were transformed using log2 (TPM + 1). Normally distributed quantitative data were presented as the mean ± standard deviation, and comparisons between groups were conducted using independent samples t-tests. Non-normally distributed quantitative data were expressed as median (P25, P75), and comparisons between groups were performed using the Mann-Whitney U test. Categorical data were reported as counts or percentages, and inter-group comparisons were conducted using the χ^2 test. Ranked data comparisons were conducted using the rank-sum test. For survival analyses, the optimal cutoff value for PRDX4 expression was determined using the 'maxstat' R package (Maximally Selected Rank Statistics, version: 0.7-25), with the minimum and maximum sample sizes per group set at >25 and <75%, respectively, to minimize bias. Statistical significance was set at P<0.05. Receiver Operating Characteristic (ROC) curve analysis was performed using the R package pROC (https://xrobin.github.io/pROC/; version 1.18.0) to evaluate the diagnostic performance of PRDX4 expression. The AUC and optimal cutoff (Youden index) were calculated.

To expand the clinical correlation analysis beyond TNM staging, the association between PRDX4 expression and two other clinicopathological features, histologic grade (tumor differentiation) and tumor size, was additionally evaluated using data from the TCGA ESCA dataset. Histologic grade was categorized according to the WHO classification as Grade I (well differentiated), Grade II (moderately differentiated), Grade III (poorly differentiated), or Grade IV/GX (undifferentiated/unknown). Tumor size was defined as the maximum diameter of the primary tumor and stratified using a 4-cm cutoff. PRDX4 high- and low-expression groups were determined by the optimal cutoff from the maxstat R package. Differences in histologic grade distribution between groups were assessed using the Wilcoxon rank-sum test, and differences in tumor size distribution were assessed using the χ^2 test. Statistically significant difference was set at P<0.05. Detailed results are presented in Table SI.

Results

Pan-cancer analysis of PRDX4. Analysis using the UALCAN database showed that PRDX4 expression was significantly upregulated in 18 tumor types, including bladder urothelial carcinoma (BLCA), breast invasive carcinoma (BRCA), cervical squamous cell carcinoma and endocervical adenocarcinoma (CESC), cholangiocarcinoma, colon adenocarcinoma (COAD) and ESCA, and significantly downregulated in kidney chromophobe (KICH) and pheochromocytoma and paraganglioma (Fig. 1A). Expression differences between tumor and normal tissues across cancers were analyzed using the SANGERBOX database. Significant differences determined by the Wilcoxon rank-sum and signed-rank tests revealed significant upregulation of PRDX4 in 30 tumor types, including glioblastoma multiforme, glioblastoma and lower-grade glioma, low-grade glioma, uterine corpus endometrial carcinoma, BRCA, CESC, lung adenocarcinoma, ESCA, stomach and esophageal carcinoma, KIPAN (KICH, KIRC and KIRP), COAD, colon adenocarcinoma and rectum adenocarcinoma, prostate adenocarcinoma, stomach adenocarcinoma, head and neck squamous cell carcinoma, kidney renal clear cell carcinoma, lung squamous cell carcinoma, liver hepatocellular carcinoma, Wilms tumor, skin cutaneous melanoma, BLCA, thyroid carcinoma, rectum adenocarcinoma, ovarian cancer, tenosynovial giant cell tumor, uterine carcinosarcoma, acute lymphoblastic leukemia, lymphangioleiomyomatosis and adrenocortical carcinoma, and significant downregulation in PAAD and KICH (Fig. 1B).

Differential expression of PRDX4 in ESCA and normal tissues. The aforementioned pan-cancer expression profiling positioned PRDX4 within the tumor landscape, indicating its potential as a tumor biomarker. Given the highly lethal nature of ESCA, a gastrointestinal malignancy with limited therapeutic options, identifying novel molecular targets is clinically significant. Therefore, the role of PRDX4 was validated and explored specifically in ESCA. Analysis using the

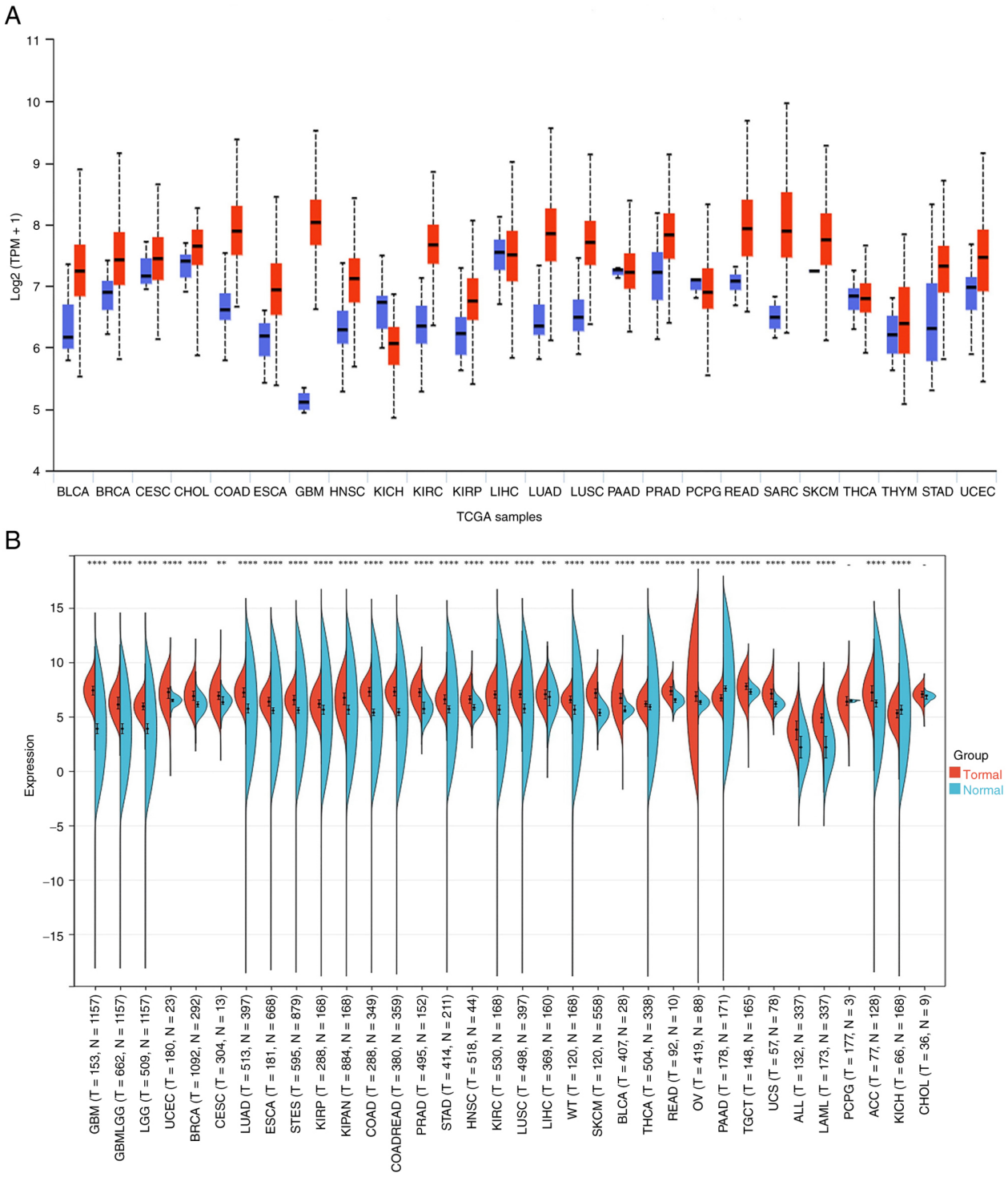

Figure 1. Pan-cancer analysis of PRDX4 expression. (A) Analysis using the UALCAN database showing PRDX4 expression across various cancer types. (B) Analysis using the SANGERBOX database further validating the differential expression of PRDX4 in a broader range of cancer types Tumor (T)=181, Normal (N)=668. Statistical significance was determined using the Wilcoxon rank-sum test. **P<0.01, ***P<0.001 and ****P<0.0001. Red represents tumor tissues, and blue represents normal tissues. Error bars indicate the standard deviation. TCGA, The Cancer Genome Atlas; BLCA, bladder urothelial carcinoma; BRCA, breast invasive carcinoma; CESC, cervical squamous cell carcinoma and endocervical adenocarcinoma; CHOL, cholangiocarcinoma; COAD, colon adenocarcinoma; ESCA, esophageal carcinoma; GBM, glioblastoma multiforme; HNSC, head and neck squamous cell carcinoma; KICH, kidney chromophobe; KIRC, kidney renal clear cell carcinoma; KIRP, kidney renal papillary cell carcinoma; LIHC, liver hepatocellular carcinoma; LUAD, lung adenocarcinoma; LUSC, lung squamous cell carcinoma; PAAD, pancreatic adenocarcinoma; PRAD, prostate adenocarcinoma; PCPG, pheochromocytoma and paraganglioma; READ, rectum adenocarcinoma; SARC, sarcoma; SKCM, skin cutaneous melanoma; THCA, thyroid carcinoma; THYM, thymoma; STAD, stomach adenocarcinoma; UCEC, uterine corpus endometrial carcinoma; TPM, transcripts per million.

SANGERBOX database revealed significantly higher PRDX4 expression in tumor tissues (n=181) compared with normal tissues (n=668) (P<0.05). Consistently, analysis using the UALCAN database also demonstrated significantly elevated PRDX4 expression in tumor tissues (n=184) relative to normal tissues (n=11) (P<0.05; Fig. 2A and B).

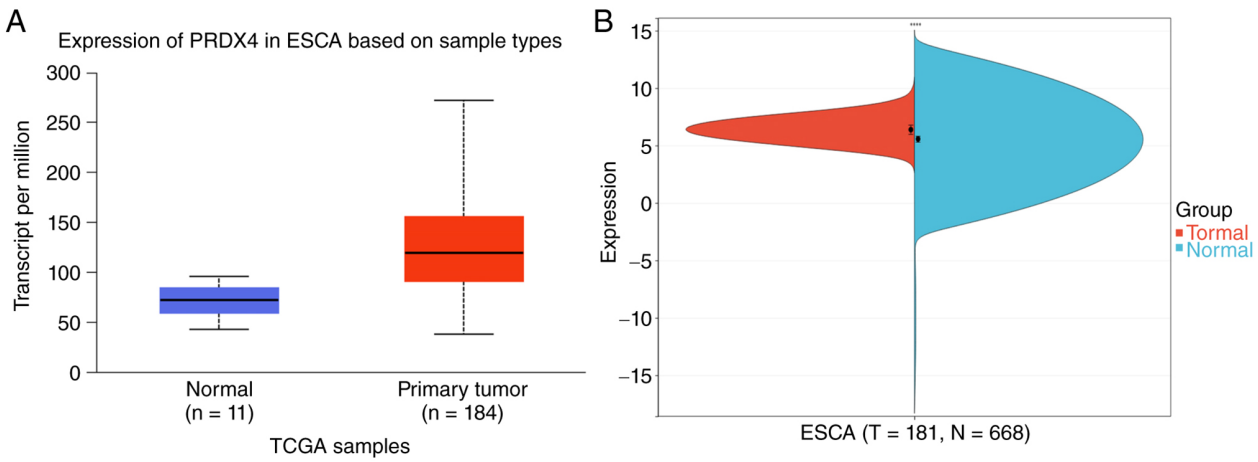

Figure 2. Differential expression analysis of PRDX4 in tumor and non-tumor tissues. (A) UALCAN database analysis showing significantly higher PRDX4 expression in ESCA tumor tissues (n=184) compared with normal tissues (n=11). (B) SANGERBOX database analysis confirming the upregulation of PRDX4 in ESCA tumor tissues (n=181) vs. normal tissues (n=668). Data are presented as the mean ± SD. Statistical significance was assessed using the Mann-Whitney U test. P<0.0001. PRDX4, peroxiredoxin 4; ESCA, esophageal cancer.

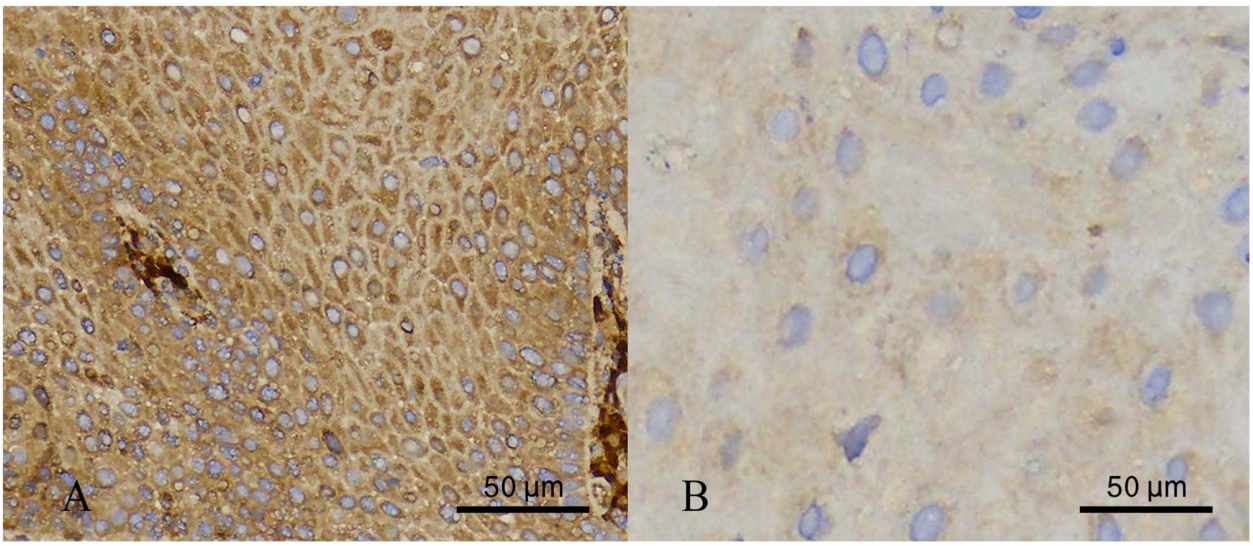

Figure 3. Immunohistochemical validation of PRDX4 protein expression. Representative images showing PRDX4 staining in (A) ESCA tumor tissue and (B) normal esophageal mucosal tissue. PRDX4 protein was predominantly localized in the cytoplasm. Strong positive staining (brown) was observed in tumor tissues, whereas normal tissues showed weak or no staining. Scale bar, 50 μm. IHC scores were significantly higher in tumor tissues (all 60 cases strongly positive) compared with normal tissues (11/60 strongly positive, P<0.05, chi-square test). PRDX4, peroxiredoxin 4.

IHC results. IHC analysis showed cytoplasmic localization of PRDX4, with significantly higher expression in ESCA compared with adjacent normal tissues (P<0.05; Fig. 2). Among 60 tumor specimens, all demonstrated strong positive staining (100% strongly positive). By contrast, only 11 of 60 normal esophageal mucosal tissues (18.33%) exhibited strong positive staining, representing a statistically significant difference (P<0.05; Fig. 3A and B).

Relationship between PRDX4 and prognosis in patients with ESCA. The optimal cutoff values for PRDX4 were calculated using the R package maxstat, dividing patients into high- and low-risk groups. Prognostic differences between these groups were further analyzed using the survfit function from the R survival package, and the log-rank test was employed to assess statistical significance. Significant differences were found in OS, PFI and DSS (P<0.05), whereas no significant difference was observed in DFI (P=0.35) (Fig. 4A-D).

The relationship between PRDX4 expression and prognosis in ESCA was analyzed using the UALCAN database. A comparison between 46 patients with ESCA with high PRDX4 expression and 138 patients with low expression indicated a significantly poorer prognosis in the high-expression group compared with the low-expression group (P<0.0001). Female patients with low PRDX4 expression demonstrated the best prognosis, while male patients with high PRDX4 expression exhibited the worst prognosis. Differences between groups were statistically significant (P=0.00032) (Fig. 5A and B).

Clinical staging and gene expression analysis. Gene expression differences across distinct clinical stages were analyzed using R software (version 3.6.4). For comparisons among multiple

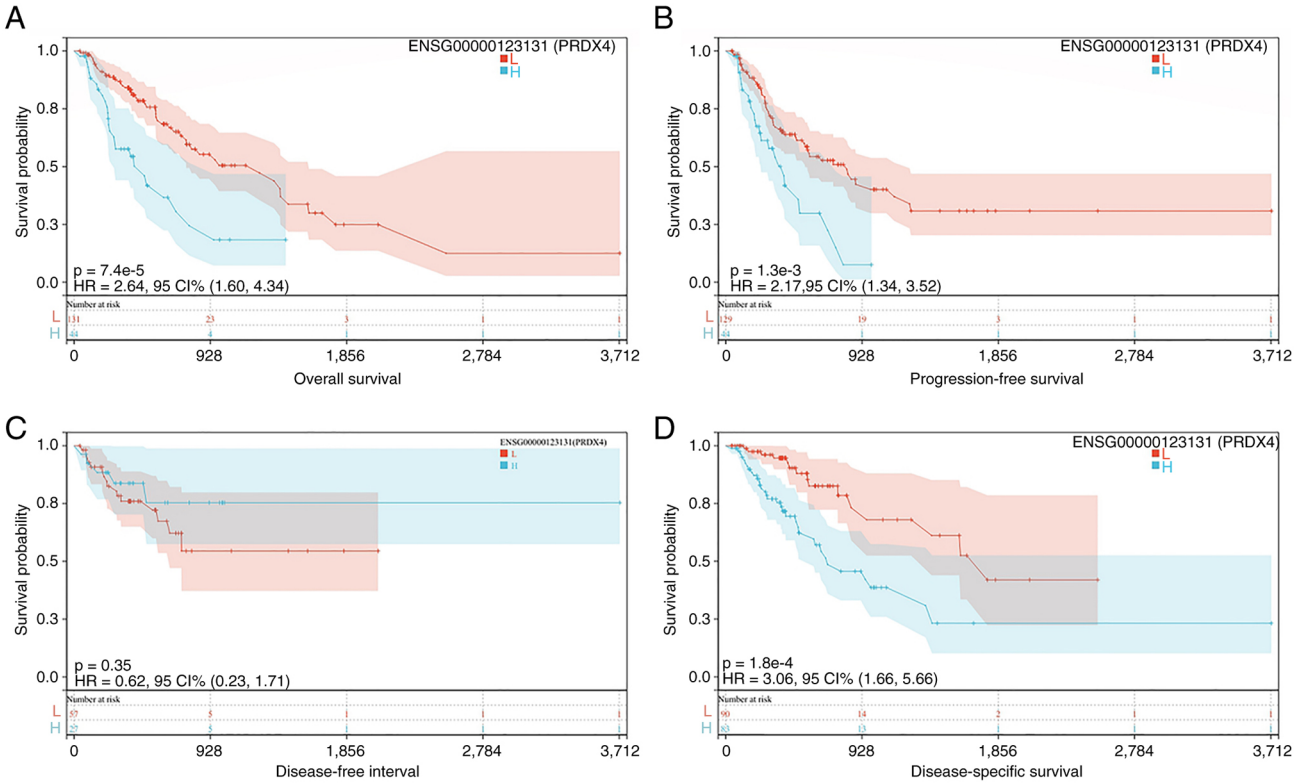

Figure 4. Prognostic value of PRDX4 in ESCA using SANGERBOX database. Kaplan-Meier survival curves demonstrating the relationship between PRDX4 expression and (A) OS, (B) PFI, (C) DFI and (D) DSS. The optimal cutoff values were determined using the maxstat R package. High PRDX4 expression was significantly associated with poorer OS, PFI and DSS (log-rank test, P<0.05), but not with DFI (P=0.35). The number of patients at risk in each group is shown below the curves. PRDX4, peroxiredoxin 4; ESCA, esophageal cancer; OS, overall survival; PFI, progression-free interval; DFI, disease-free interval; DSS, disease-specific survival; HR, hazard ratio; CI, confidence interval.

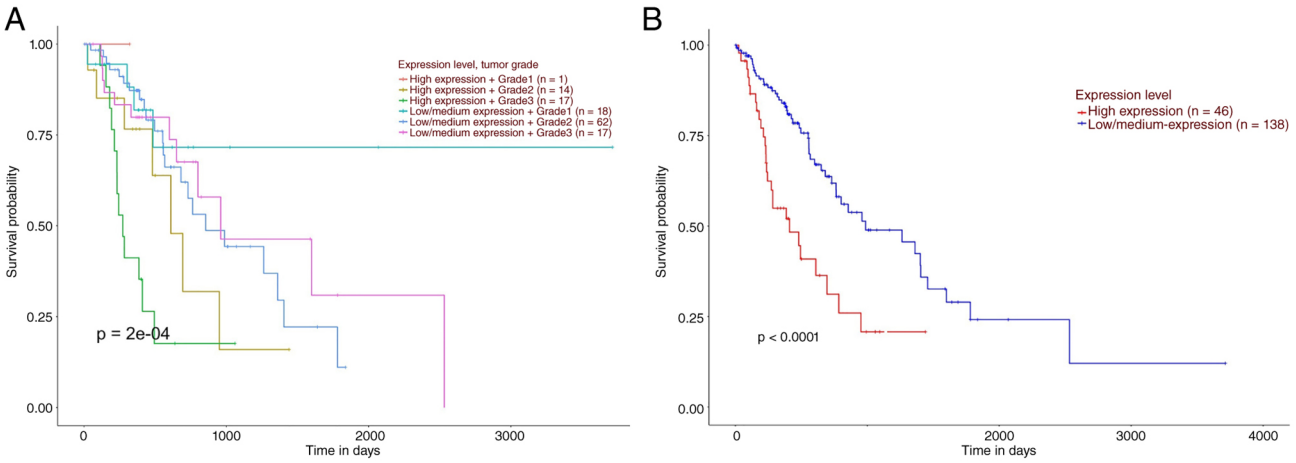

Figure 5. Survival analysis of PRDX4 in ESCA using UALCAN database. (A) Kaplan-Meier survival curves stratified by tumor grade and PRDX4 expression level. Patients with high PRDX4 expression and Grade 3 tumors exhibited the worst prognosis, while those with low/medium PRDX4 expression and Grade 1 tumors had the best prognosis (P=2e-04, log-rank test). (B) Kaplan-Meier survival curves comparing patients with high (n=46) versus low/medium (n=138) PRDX4 expression. High PRDX4 expression was associated with significantly poorer overall survival (P<0.0001, log-rank test). PRDX4, peroxiredoxin 4; ESCA, esophageal cancer.

groups, one-way analysis of variance (ANOVA) was performed, followed by Tukey's honestly significant difference (HSD) post hoc test for multiple pairwise comparisons. Unpaired Student's t-test was used only for comparisons between two specific groups where applicable. Comparison of PRDX4 expression levels among patients with ESCA across different TNM stages revealed no significant differences in T or M stages. However, significant differences in PRDX4 expression were observed among different N stages (P=0.006) (Table I). Furthermore, the clinicopathological correlation analysis was extended to include tumor differentiation and tumor size. As shown in Table SI, PRDX4 expression was significantly associated with tumor differentiation grade (P=0.028), with higher expression observed in poorly differentiated tumors. Although

Table I. Comparison of PRDX4 expression levels in patients with different TNM stages.

Characteristics	Expression level of PRDX4 (n=81)		P-value
	Low (%)	High (%)	
Pathologic T stage, n (%)			0.372
T1	16 (11)	11 (7.6)	
T2	23 (15.9)	14 (9.7)	
T3 and T4	40 (27.6)	41 (28.3)	
Pathologic N stage, n (%)			0.006
N0	42 (29.2)	24 (16.7)	
N1	25 (17.4)	38 (26.4)	
N2	8 (5.6)	1 (0.7)	
N3	4 (2.8)	2 (1.4)	
Pathologic M stage, n (%)			
M0	66 (51.2)	55 (42.6)	0.569
M1	3 (2.3)	5 (3.9)	

T, tumor; N, node; M, metastasis.

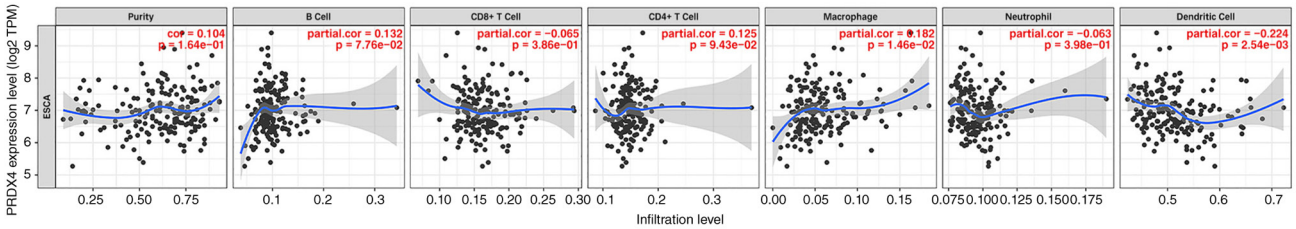

Figure 6. Correlation between PRDX4 expression and immune cell infiltration using TIMER database. Scatter plots showing the correlation between PRDX4 expression and infiltration levels of six immune cell types in esophageal cancer. PRDX4 expression showed significant positive correlations with infiltration of macrophages (R=0.312, P=0.003) and dendritic cells (R=0.286, P=0.007). No significant correlations were observed with B cells, CD4$^+$ T cells, CD8$^+$ T cells, or neutrophils. Tumor purity was also assessed. Statistical significance was determined by partial correlation analysis after adjusting for tumor purity. PRDX4, peroxiredoxin 4.

not statistically significant, there was a trend towards higher PRDX4 expression in larger tumors (P=0.061).

ROC curve analysis for diagnostic evaluation. To evaluate the potential diagnostic value of PRDX4 in distinguishing ESCA from normal tissues, ROC curve analysis was performed using the TCGA ESCA dataset. The area under the curve (AUC) was calculated to assess the overall diagnostic performance. As shown in Fig. S1, the ROC curve yielded an AUC of 0.969, indicating excellent discriminatory ability. At the optimal cutoff point determined by the Youden index, the sensitivity and specificity were 98.0 and 94.0%, respectively. These results suggest that PRDX4 expression has a strong capacity to differentiate ESCA tissues from normal esophageal tissues, supporting its potential as a diagnostic biomarker, although further validation in independent cohorts is warranted.

Relationship between PRDX4 and immune infiltration. The association between tumor progression and immune cell infiltration (B cells and macrophages) was analyzed using the TIMER database. Additionally, analysis using the STRING database revealed that PRDX4 expression correlated significantly with the immune infiltration of DCs and macrophages, whereas no associations were observed with B cells, tumor purity, CD4$^+$ T cells, CD8$^+$ T cells, or neutrophils (P>0.05) (Fig. 6).

The deconvo_CIBERSOR method from the R package IOBR (version 0.99.9; https://www.ncbi.nlm.nih.gov/pmc/articles/PMC8283787/) was utilized to evaluate immune cell infiltration scores in tumor patients based on gene expression. Immune cells analyzed included naive B cells, memory B cells, plasma cells, CD8$^+$ T cells, naive CD4$^+$ T cells, resting memory CD4$^+$ T cells, activated memory CD4$^+$ T cells, follicular helper T cells, regulatory T cells (Tregs), gamma-delta T cells, resting NK cells, activated NK cells, monocytes, macrophages (M0, M1, M2), resting DCs, activated DCs, resting mast cells, activated mast cells, eosinophils and neutrophils. Subsequently, the corr.test function from the psych package (version 2.1.6) in R was employed to calculate Pearson's correlation coefficients between gene expression and immune cell infiltration scores across tumor samples, identifying significant correlations. Results revealed significant correlations between PRDX4 expression in ESCA and infiltration by CD8$^+$ T cells, resting memory CD4$^+$ T cells, Tregs, M1 macrophages and activated mast cells (Fig. 7).

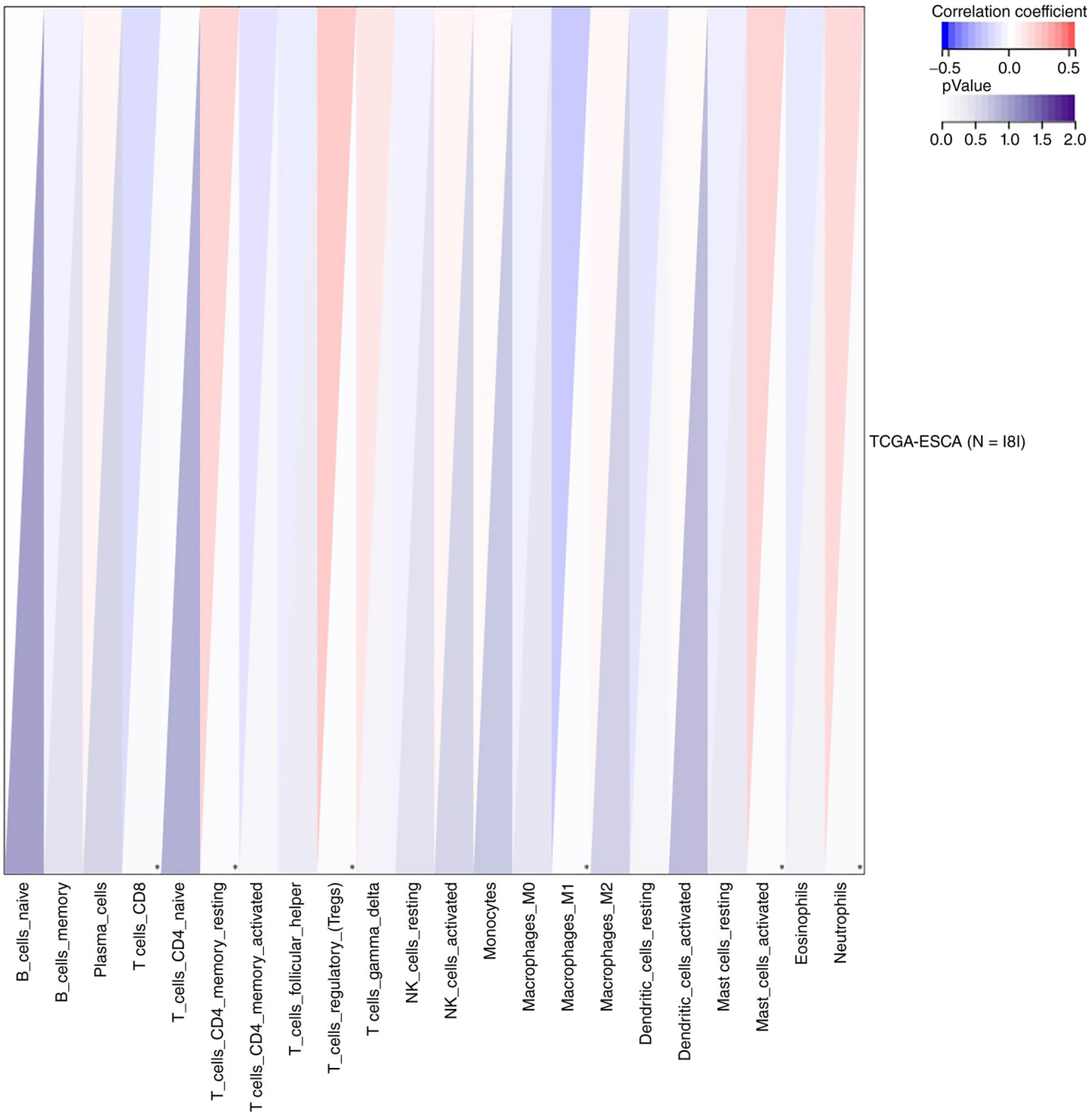

Figure 7. Correlation between PRDX4 expression and immune cell infiltration using CIBERSORT algorithm. Heatmap and scatter plots showing the correlation between PRDX4 expression and the relative proportions of 22 immune cell subtypes in ESCA. Significant correlations were identified with $CD8^+$ T cells, resting memory $CD4^+$ T cells, Tregs, M1 macrophages and activated mast cells (Pearson correlation, $^*P<0.05$). Red indicates positive correlation, and blue indicates negative correlation. The strength of the correlation is represented by the color intensity. Sample sizes: TCGA-ESCA cohort (n=181). Statistics: Spearman correlation analysis. PRDX4, peroxiredoxin 4; ESCA, esophageal cancer; NK, natural killer cells; Treg, regulatory T cells; M0/M1/M2, macrophage subtypes; cor, correlation coefficient.

Enrichment analysis. Gene Ontology (GO) and Kyoto Encyclopedia of Genes and Genomes (KEGG) analyses are widely used bioinformatics approaches for classifying genes or proteins by function and associating them with biological processes or metabolic pathways, providing insights into their roles within cells. GO analysis indicated that PRDX4 regulation in ESCA was significantly associated with the following pathways: Mitochondrial part, mitochondrion, mitochondrial matrix, mitochondrial protein complex, inner mitochondrial membrane protein complex, ribose phosphate metabolic process, small molecule metabolic process, sulfur compound metabolic process, catalytic complex, and intrinsic component of mitochondrial inner membrane. KEGG analysis revealed associations between PRDX4 regulation in ESCA and pathways including the glucagon signaling pathway, carbon metabolism, protein export, citrate cycle [tricarboxylic acid (TCA) cycle], pentose phosphate pathway, beta-alanine metabolism, metabolic pathways, DNA replication, pyruvate metabolism, and porphyrin and chlorophyll metabolism (Fig. 8A and B).

Kaplan-Meier plotter database. The prognostic significance of PRDX4 in patients with ESCA was assessed using the

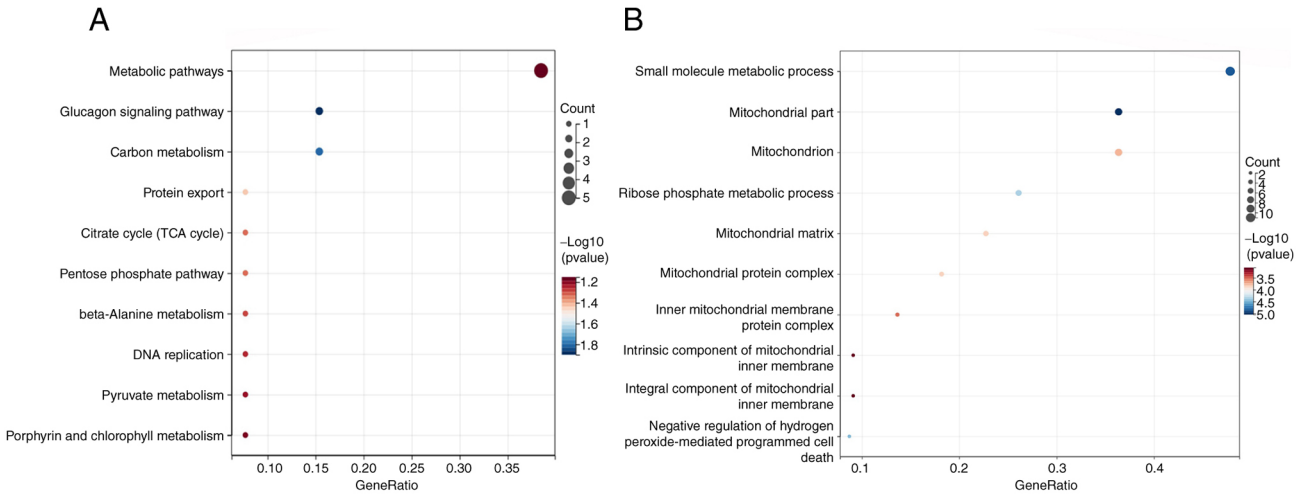

Figure 8. Functional enrichment analysis of peroxiredoxin 4-coexpressed genes in esophageal cancer. (A) Gene Ontology analysis showing enrichment of biological processes, cellular components, and molecular functions related to mitochondrial function, metabolic processes and catalytic activity. (B) Kyoto Encyclopedia of Genes and Genomes pathway analysis revealing associations with metabolic pathways, including the TCA cycle, carbon metabolism and pyruvate metabolism. The top 10 significantly enriched terms (P<0.05) are displayed. The size of the circles represents the number of genes enriched, and the color represents the P-value (red indicating lower P-values). GeneRatio, enrichment ratio; TCA, tricarboxylic acid cycle. Statistics: Hypergeometric distribution test (P-values adjusted).

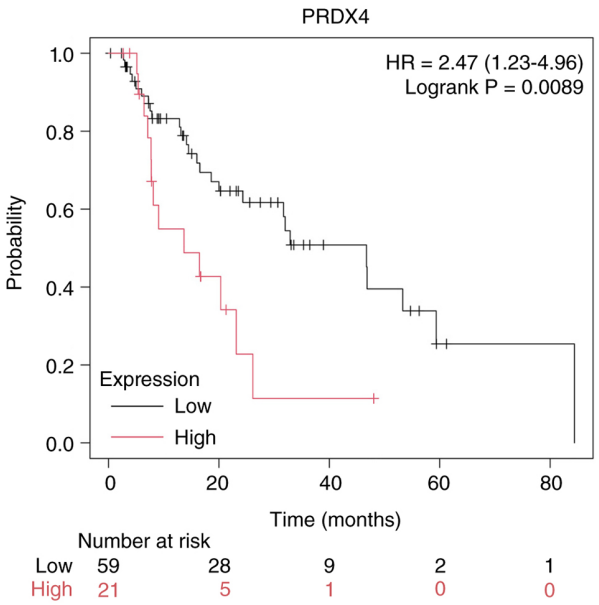

Figure 9. Kaplan-Meier plot from the Kaplan-Meier Plotter database. Survival curve demonstrating that high PRDX4 expression predicts poor overall survival in patients with esophageal cancer (HR=1.56, 95% CI=1.12-2.18, log-rank P=0.0089). The optimal cutoff was determined automatically by the database. The number of patients at risk at different time points is shown below the graph. Sample sizes: Risk table below shows numbers at risk (Low: initial n=59; High: initial n=21). Statistics: Log-rank test. Significance: P=0.0089 (Log rank P), HR=2.47 (95% CI=1.23-4.96); P<0.05 was considered to indicate a statistically significant difference. PRDX4, peroxiredoxin 4; HR, hazard ratio; CI, confidence interval.

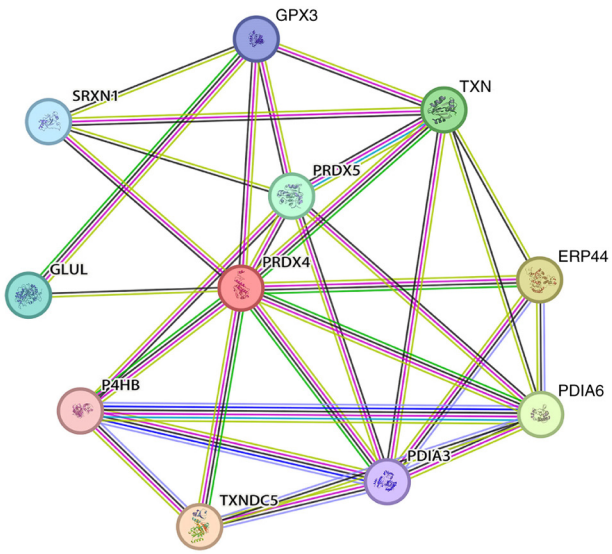

Figure 10. Protein-protein interaction network of PRDX4. Analysis using the STRING database revealed a network of proteins interacting with PRDX4, including GPX3, TXN and other antioxidant-related proteins. The thickness of the connecting lines represents the confidence score of the interaction. Nodes represent proteins, and edges represent predicted or experimentally validated functional associations. PRDX, peroxiredoxin; GPX3, glutathione peroxidase 3; TXNDC5, thioredoxin domain containing 5; P4HB, prolyl 4-hydroxylase subunit beta; GLUL, glutamate-ammonia ligase; SRXN1, sulfiredoxin 1; TXN, thioredoxin; ERP44, endoplasmic reticulum protein 44; PDIA6, protein disulfide isomerase family A member 6; PDIA3, protein disulfide isomerase family A member 3.

Kaplan-Meier Plotter database. Patients were classified into high- and low-expression groups based on gene expression levels at various quantiles. Kaplan-Meier survival curves were plotted to compare the two groups, and the hazard ratio (HR), 95% confidence interval (CI) and log-rank P-value were calculated. The results demonstrated that PRDX4 has significant prognostic value in patients with ESCA (P=0.0089; Fig. 9).

PPI analysis. Proteins typically exert their biological functions through interactions with other proteins. Analyzing PPI networks enhances the understanding of intracellular functional regulation and signaling pathways. Thus, interaction analyses using the STRING database revealed multiple proteins interacting with PRDX4, including GPX3 and TXN (Fig. 10).

Discussion

The present study systematically investigated the expression characteristics, clinical significance and potential molecular mechanisms of PRDX4 in ESCA. By integrating multi-omics bioinformatics analyses and validating findings with tissue samples, a series of consistent and mutually reinforcing results were obtained. First, both pan-cancer analysis and ESCA-specific analyses demonstrated widespread upregulation of PRDX4 across multiple tumor types, including ESCA, suggesting its pleiotropic tumor-promoting role. IHC validation in an independent clinical cohort further confirmed elevated cytoplasmic PRDX4 protein expression in tumors. The consistency between transcriptomic and proteomic analyses significantly increased the reliability of these findings and indicated that PRDX4 overexpression may represent a stable molecular feature of ESCA.

Second, prognostic analyses revealed a significant correlation between elevated PRDX4 expression and poorer OS, PFI and DSS in patients with ESCA, indicating that PRDX4 may serve as an independent risk factor for long-term patient outcomes. Notably, PRDX4 showed no significant correlation with DFI, suggesting its role may primarily involve promoting tumor progression and metastasis rather than initiating tumor recurrence. This interpretation aligns with clinical staging analysis, which demonstrated significant associations between PRDX4 expression and lymph node (N) staging, but not tumor (T) or distant metastasis (M) staging. The additional correlation with poorer tumor differentiation further supports its association with aggressive tumor behavior. These findings strongly support the hypothesis that PRDX4 specifically promotes lymph node metastasis in ESCA, providing critical clinical evidence for its 'metastasis-promoting' function and explaining its association with poor OS and DSS.

Third, tumor microenvironment (TME) analysis offered insights into potential mechanisms underlying the influence of PRDX4 on prognosis. In the present study, a positive correlation was observed between PRDX4 expression and infiltration of myeloid immune cells, particularly macrophages and DCs. Tumor-associated macrophages (TAMs), especially M2-type TAMs, are known to facilitate tumor progression by suppressing immune responses and promoting angiogenesis and metastasis. Therefore, PRDX4 may contribute to an immunosuppressive microenvironment and tumor progression by regulating the redox status of tumor cells or secreting specific cytokines, thereby promoting lymph node metastasis and leading to poorer prognosis (18,19).

Beyond macrophages, the current correlation analyses revealed a significant positive association between PRDX4 expression and DC infiltration in ESCA, a finding that warrants mechanistic consideration. DCs are central to antitumor immunity through antigen presentation and T-cell priming, yet their function is highly susceptible to the TME. Although the present data demonstrate a statistical correlation, the underlying mechanisms remain hypothetical and require experimental validation. It is proposed that PRDX4 may influence DC recruitment and function through at least three interconnected pathways. First, as a secreted antioxidant enzyme, PRDX4 can modulate extracellular redox balance. Elevated PRDX4 in the TME may reduce oxidative stress, thereby diminishing the release of damage-associated molecular patterns that typically act as chemo-attractants for immature DCs. This could paradoxically impair DC recruitment while protecting tumor cells from oxidative damage. Second, intracellular PRDX4 within tumor cells regulates mitochondrial reactive oxygen species (ROS) production. Given that mitochondrial metabolism and ROS signaling are critical for DC maturation and cytokine secretion, PRDX4-mediated alterations in tumor cell metabolism, particularly through the TCA cycle and pyruvate metabolism as suggested by our KEGG analysis, may lead to the release of metabolic intermediates (for example, lactate and succinate) that suppress DC differentiation or promote a tolerogenic phenotype. Third, PRDX4 may directly interact with or regulate redox-sensitive transcription factors (for example, NF-κB and NRF2) in tumor cells, influencing the secretion of chemokines such as CCL4, CCL5, or CXCL10 that are known to govern DC trafficking. It is crucial to emphasize that these proposed mechanisms are speculative and derived from the known biochemical functions of PRDX4 and general principles of tumor immunology. They are not directly evidenced by our current correlation analyses, which only establish an association, not causation, between PRDX4 transcript levels and DC infiltration estimates from deconvolution algorithms. Future studies employing DC-tumor cell co-culture systems, PRDX4 genetic manipulation, and *in vivo* DC depletion models are indispensable to test these hypotheses and determine whether the observed correlation reflects a causal immunomodulatory role of PRDX4 or merely an epiphenomenon of tumor progression.

However, the lack of correlation between PRDX4 expression and $CD8^+$ T cell infiltration suggests that PRDX4 may not directly influence adaptive immune effector cells, with its immunomodulatory effects possibly restricted to the innate immune compartment (20,21).

In addition to its prognostic value, the ROC analysis of the present study demonstrated that PRDX4 expression can effectively discriminate ESCA from normal tissues with a high AUC of 0.969, suggesting considerable diagnostic potential. However, it is acknowledged that ROC performance based on a single dataset may be optimistic, and the true diagnostic utility requires prospective evaluation in large, multi-center screening cohorts. Therefore, while PRDX4 shows promise as a diagnostic adjunct, its primary clinical value in the current study remains as a prognostic indicator, as reflected by the consistent survival and clinicopathological associations.

It is important to note the apparent discrepancies between the immune infiltration results obtained from the TIMER and CIBERSORT algorithms. TIMER analysis primarily showed associations with macrophages and DCs, while CIBERSORT revealed broader correlations with $CD8^+$ T cells, Tregs and M1 macrophages. These differences are likely attributable to the distinct computational principles of each method. TIMER uses a partial correlation approach that adjusts for tumor purity and estimates abundance for only six immune cell types, whereas CIBERSORT employs a deconvolution algorithm based on a curated gene expression signature matrix (LM22) to estimate the relative proportions of 22 immune cell subtypes (14,17). The discrepancy highlights the importance of using multiple algorithms to cross-validate findings and suggests that PRDX4 may exert its immunomodulatory effects through a

complex network involving both innate and adaptive immune components, with the specific associations being dependent on the analytical resolution and the reference datasets used.

Fourth, functional enrichment analysis further highlighted a close association between PRDX4 and mitochondrial functions, as well as multiple metabolic pathways, including carbon metabolism, the TCA cycle and pyruvate metabolism. As an antioxidant protein, PRDX4 plays a crucial role in maintaining cellular redox homeostasis, which is tightly linked to cellular metabolism, particularly mitochondrial energy metabolism (22,23). The enrichment of mitochondrial pathways suggests that PRDX4 may be pivotal in managing the oxidative stress generated by active mitochondrial respiration in rapidly proliferating tumor cells. Furthermore, its association with metabolic pathways such as the TCA cycle and carbon metabolism suggests that PRDX4 might facilitate the metabolic reprogramming known as the 'Warburg effect', where cancer cells shift to aerobic glycolysis. By neutralizing ROS produced during enhanced mitochondrial activity, PRDX4 could protect tumor cells from oxidative damage, thereby sustaining their survival and proliferation. These findings suggest that the oncogenic role of PRDX4 in ESCA might be mediated by its ability to remodel tumor cell metabolism, thereby satisfying the energetic and biosynthetic demands of rapidly proliferating tumor cells. Thus, PRDX4 may act as a 'metabolic guardian' during tumor metabolic reprogramming, a hallmark feature of cancer. This metabolic role may also explain its association with immune infiltration, as metabolic byproducts can influence the polarization and function of immune cells, particularly macrophages.

Comparing the present findings with previous studies in other cancers, PRDX4 overexpression has been linked to poor prognosis in gastric and breast cancers, suggesting a conserved oncogenic role across malignancies (8-10,17). However, the present study is the first to comprehensively demonstrate its specific correlation with lymph node metastasis and metabolic pathways in ESCA, differentiating it from prior work that primarily focused on proliferation mechanisms via non-coding RNAs. While a recent study identified the THUMPD3-AS1/miR-29a-3p/ELK1/PRDX4 axis in ESCA cells (11), the present study complements this by providing the clinical and translational context, validating its prognostic power and revealing its association with the TME and metabolism in patient cohorts.

Finally, PPI network analysis revealed strong interactions between PRDX4 and other critical antioxidant proteins, such as GPX3 and TXN, supporting the hypothesis that PRDX4 functions within a coordinated antioxidant network to collectively counteract excessive oxidative stress in ESCA cells, thereby maintaining their survival advantage (24). Independent validation using the Kaplan-Meier Plotter database further strengthened the value of PRDX4 as a prognostic biomarker in ESCA.

Several limitations of the present study should be acknowledged. First, the sample size for IHC validation (n=60) is relatively small and derived from a single center. Larger, multicenter cohorts are necessary to confirm the clinical utility of PRDX4 as a biomarker. Second, while the clinicopathological correlation was expanded, data on treatment response were not available, limiting our assessment of PRDX4's predictive value for therapy. Third, the mechanistic insights are based entirely on bioinformatic predictions and correlation analyses. Direct *in vitro* and *in vivo* functional studies, such as PRDX4 overexpression/knockdown assays to examine its impact on cell proliferation, migration, metabolism and immune cell interaction, are essential to validate the proposed mechanisms. These experiments will be the focus of our future research.

In conclusion, the present study systematically characterized the multifaceted oncogenic roles of PRDX4 in ESCA through multi-dimensional analyses. First, PRDX4 was significantly overexpressed in tumor tissues. Second, its overexpression was closely correlated with lymph node metastasis and poor prognosis. Third, the underlying mechanisms may involve metabolic reprogramming of tumor cells (particularly mitochondrial metabolic pathways) and modulation of the TIME (especially infiltration of myeloid immune cells). The novelty of the present study lies in providing a comprehensive clinical and bioinformatic characterization of PRDX4 in ESCA, bridging the gap between mechanistic studies and clinical translation. PRDX4 was established not merely as a molecule of interest, but as a clinically relevant prognostic biomarker and a potential node in the metabolism-immunity crosstalk. These findings not only establish PRDX4 as a potential prognostic biomarker in ESCA but also identify a novel mechanism of tumor progression mediated via the 'metabolism-immunity' axis, providing essential theoretical support for future therapeutic strategies targeting PRDX4 and its associated pathways. The present findings suggest that PRDX4 may serve as a promising prognostic biomarker and a potential therapeutic target for ESCA. Future studies should directly verify the precise molecular mechanisms by which PRDX4 regulates ESCA cell metabolism, mediates immune evasion, and promotes lymph node metastasis using *in vivo* and *in vitro* experimental approaches.

Acknowledgements

Not applicable.

Funding

No funding was received.

Availability of data and materials

The data generated in the present study may be requested from the corresponding author.

Authors' contributions

XL contributed to the study conception and design, performed the formal analysis and investigation, curated the data, created the visualizations, and drafted the original manuscript. LP contributed to the methodology development, validation, provision of resources, supervision of the project, project administration, and acquisition of funding, and critically reviewed and edited the manuscript. HS provided resources, conducted investigation and curated data. WP curated data and conducted project administration. All authors read and approved the final version of the manuscript. XL and WP confirm the authenticity of all the raw data.

Ethics approval and consent to participate

The present study was conducted in accordance with the declaration of Helsinki. The present study was approved by the Ethics Committee of Ningxia Medical University General Hospital (approval no. KYLL-2026-0022; Yinchuan, China). A written informed consent was obtained from all participants.

Patient consent for publication

Not applicable.

Competing interests

The authors declare that they have no competing interests.

References

1. Zhang Z, Wang Y, Liu Y, Wu H, Xu X, Wang K, He C and Qian C: Involvement of the PRDX family and its clinical functions in different types of gastrointestinal cancer (review). Oncol Rep 54: 90, 2025.
2. Li Q, Dou W, Qi J, Qin X, Chen S and He Y: Genomewide analysis of the CIII peroxidase family in sweet orange (Citrus sinensis) and expression profiles induced by Xanthomonas citri subsp. citri and hormones. J Genet 99: 10, 2020.
3. Bai Z, Yin W, Liu R, Tang M, Shi X, Luo C and Xie X: PRDX1 Cys52Ser variant alleviates nonalcoholic steatohepatitis by reducing inflammation in mice. Mol Metab 76: 101789, 2023.
4. Yamaguchi R, Guo X, Zheng J, Zhang J, Han J, Shioya A, Uramoto H, Mochizuki T and Yamada S: PRDX4 improved aging-related delayed wound healing in mice. J Invest Dermatol 141: 2720-2729, 2021.
5. Lin Y, Totsuka Y, He Y, Kikuchi S, Qiao Y, Ueda J, Wei W, Inoue M and Tanaka H: Epidemiology of esophageal cancer in Japan and China. J Epidemiol 23: 233-242, 2013.
6. Okada G, Matsumoto Y, Habu D, Matsuda Y, Lee S and Osugi H: Relationship between GLIM criteria and disease-specific symptoms and its impact on 5-year survival of esophageal cancer patients. Clin Nutr 40: 5072-5078, 2021.
7. Qiao X, Cheng Z, Xue K, Xiong C, Zheng Z, Jin X and Li J: Tumor-associated macrophage-derived exosomes LINC01592 induce the immune escape of esophageal cancer by decreasing MHC-I surface expression. J Exp Clin Cancer Res 42: 289, 2023.
8. Zhang L, Wu K, Hou Y and Li X: Validation of the interaction between PRDX4 and TXNDC5 in gastric cancer and the significance of the PRDX4 gene in gastric cancer based on a data mining analysis. Transl Cancer Res 13: 81-101, 2024.
9. Jiang W, Wang M, Chen Q, Yu X, Liu G, He X, Mei C and Ou C: Immune infiltration related PRDX4 facilitates the malignant features and drug resistance of breast cancer. Sci Rep 15: 27507, 2025.
10. Jain P, Dvorkin-Gheva A, Mollen E, Malbeteau L, Xie M, Jessa F, Dhavarasa P, Chung S, Brown KR, Jang GH, *et al*: NOX4 links metabolic regulation in pancreatic cancer to endoplasmic reticulum redox vulnerability and dependence on PRDX4. Sci Adv 7: eabf7114, 2021.
11. Tang M, Sun J and Cai Z: LncRNA THUMPD3-AS1 promotes the proliferation and migration of esophageal cancer cells through the miR-29a-3p/ELK1/PRDX4 signaling pathway. Semin Oncol 52: 152350, 2025.
12. Chandrashekar DS, Bashel B, Balasubramanya SAH, Creighton CJ, Ponce-Rodriguez I, Chakravarthi BVSK and Varambally S: UALCAN: A portal for facilitating tumour subgroup gene expression and survival analyses. Neoplasia 19: 649-658, 2017.
13. Shen W, Song Z, Zhong X, Huang M, Shen D, Gao P, Qian X, Wang M, He X, Wang T, *et al*: Sangerbox: A comprehensive, interaction-friendly clinical bioinformatics analysis platform. Imeta 1: e36, 2022.
14. Szklarczyk D, Kirsch R, Koutrouli M, Nastou K, Mehryary F, Hachilif R, Gable AL, Fang T, Doncheva NT, Pyysalo S, *et al*: The STRING database in 2023: Protein-protein association networks and functional enrichment analyses for any sequenced genome of interest. Nucleic Acids Res 51 (D1): D638-D646, 2023.
15. Attaelmanan AM, Alzubair S, Ahmmed AS, Abdelgalil A, Ali F, Khalafalla AS, Attaelmanan GA and Alfaki M: A comprehensive pan-cancer analysis reveals GRB7 as a potential diagnostic and prognostic biomarker. Cureus 16: e74907, 2024.
16. Hou GX, Liu P, Yang J and Wen S: Mining expression and prognosis of topoisomerase isoforms in non-small-cell lung cancer by using Oncomine and Kaplan-Meier plotter. PLoS One 12: e0174515, 2017.
17. Cancer Genome Atlas Research Network; Analysis Working Group: Asan University; BC Cancer Agency; Brigham and Women's Hospital; Broad Institute; Brown University; Case Western Reserve University; Dana-Farber Cancer Institute; Duke University, *et al*: Integrated genomic characterization of oesophageal carcinoma. Nature 541: 169-175, 2017.
18. Park SY, Lee YJ, Park J, Kim TH, Hong SC, Jung EJ, Ju YT, Jeong CY, Park HJ, Ko GH, *et al*: PRDX4 overexpression is associated with poor prognosis in gastric cancer. Oncol Lett 19: 3522-3530, 2020.
19. Jia R, Shi D, Li W, Yang J, Zhang Y and Han Y: New early gastric cancer marker PRDX4 promote the tumorigenesis and progression of gastric cancer via eliminating ROS. Sheng Wu Gong Cheng Xue Bao 36: 320-331, 2020 (In Chinese).
20. Lipinski S, Pfeuffer S, Arnold P, Treitz C, Aden K, Ebsen H, Falk-Paulsen M, Gisch N, Fazio A, Kuiper J, *et al*: Prdx4 limits caspase-1 activation and restricts inflammasome-mediated signaling by extracellular vesicles. EMBO J 38: e101266, 2019.
21. Lu Z, Tang Y, Qin R, Han Z, Chen H, Cao L, Zhang P, Yang X, Yu W, Cheng N and Sun Y: Revealing Prdx4 as a potential diagnostic and therapeutic target for acute pancreatitis based on machine learning analysis. BMC Med Genomics 17: 93, 2024.
22. Chen Q, Thompson J, Hu Y and Lesnefsky EJ: Endoplasmic reticulum stress and alterations of peroxiredoxins in aged hearts. Mech Ageing Dev 215: 111859, 2023.
23. Konno T, Pinho Melo E, Lopes C, Mehmeti I, Lenzen S, Ron D and Avezov E: ERO1-independent production of H2O2 within the endoplasmic reticulum fuels Prdx4-mediated oxidative protein folding. J Cell Biol 211: 253-259, 2015.
24. Druso JE, MacPherson MB, Chia SB, Elko E, Aboushousha R, Seward DJ, Abdelhamid H, Erickson C, Corteselli E, Tarte M, *et al*: Endoplasmic reticulum oxidative stress promotes glutathione-dependent oxidation of collagen-1A1 and promotes lung fibroblast activation. Am J Respir Cell Mol Biol 71: 589-602, 2024.